Synthesis and properties of $Tl_2Mn_{2-x}Ti_xO_7$ pyrochlores with colossal magnetoresistance

2001 J. Phys.: Condens. Matter 13 10991

(http://iopscience.iop.org/0953-8984/13/48/323)

INSTITUTE OF PHYSICS PUBLISHING JOURNAL OF PHYSICS: CONDENSED MATTER

J. Phys.: Condens. Matter **13** (2001) 10991–11000 PII: S0953-8984(01)27242-7

Synthesis and properties of $Tl_2Mn_{2-x}Ti_xO_7$ pyrochlores with colossal magnetoresistance

P Velasco[1], J A Alonso[1], M J Martínez-Lope[1], M T Casais[1], J L Martínez[1] and M T Fernández-Díaz[2]

[1] Instituto de Ciencia de Materiales de Madrid, CSIC, Cantoblanco, E-28049 Madrid, Spain
[2] Institut Laue–Langevin, BP 156, F-38042 Grenoble Cédex 9, France

Received 24 July 2001, in final form 7 September 2001
Published 16 November 2001
Online at stacks.iop.org/JPhysCM/13/10991

Abstract

A new series of Ti-substituted derivatives of $Tl_2Mn_2O_7$ pyrochlore have been prepared under moderate pressures ($P = 2$ GPa). Materials of nominal stoichiometry $Tl_2Mn_{2-x}Ti_xO_7$, with $0 \leqslant x \leqslant 0.4$, have been characterized by neutron powder diffraction (NPD), magnetic, magnetotransport, and Hall measurements. The Ti-substituted materials are ferromagnetic, with Curie temperatures slightly reduced with respect to that of $Tl_2Mn_2O_7$, as a result of the introduction of a non-magnetic cation into the Mn sublattice, without nominal change of valence upon doping. Unlike the undoped ($x = 0$) compound, which shows a significant thallium and oxygen deficiency in the O′ sublattice of the pyrochlore structure, the Ti-doped materials are fully stoichiometric, as deduced from NPD data. This result is consistent with the net increase observed in the number of carriers (electrons), which explains the reduction in resistivity and magnetoresistance.

1. Introduction

Colossal magnetoresistance (CMR) was first discovered in mixed-valence $La_{1-x}M_xMnO_3$ (M = Ba, Sr Ca) perovskite manganites. This effect consists of the variation of the electric resistivity upon the application of a magnetic field. The metallic conductivity below the ferromagnetic Curie temperature (T_C) is driven by a double-exchange (DE) mechanism, by virtue of which the e_g electrons gain kinetic energy by hopping from a Mn^{3+} site to another Mn^{4+} neighbour, keeping their spins parallel to those of the ferromagnetically aligned t_{2g} spins. A second important ingredient for explaining CMR in manganites is the presence of a strong electron–lattice coupling, due to the Jahn–Teller character of Mn^{3+} cations, imposing an important distortion of the MnO_6 octahedra and originating an electronic conduction via polaron hopping.

A few years ago, CMR properties were discovered in $Tl_2Mn_2O_7$ pyrochlore [1–3]. In principle, in the stoichiometric compound there is no mixed Mn^{3+}/Mn^{4+} valence, which excludes the possibility of DE and also that of a Jahn–Teller effect. $Tl_2Mn_2O_7$ crystallizes in

the cubic pyrochlore-type structure, also constituted by vertex-sharing MnO_6 octahedra, with a characteristic Mn–O–Mn bond angle close to 133°. This material is ferromagnetic (FM), with a T_C of about 120 K. Together with the magnetic transition, the material exhibits a metal–insulator transition, with a huge drop in resistivity upon cooling. Although it seems clear that the CMR properties are due to the strong spin fluctuations that appear around T_C, the mechanism responsible for the magnetic interactions and, hence, for the spin fluctuations, remains unclear. Some authors proposed a simple FM superexchange (SE) interaction between neighbouring Mn^{4+} cations, via Mn–O–Mn paths. But this simple SE model does not account for the negative T_C-shift which develops when an external pressure is applied. Subsequently, Sushko *et al* described a new scenario in which nearest-neighbour interactions are antiferromagnetic (AF), but the next-nearest-neighbour interactions are FM. Due to the geometric frustration of the pyrochlore structure, the latter dominates [4]; this is thought to explain the strange behaviour under external pressure.

Recently, Núñez-Regueiro and Lacroix [5] proposed a new model for this compound, in which an extra indirect exchange effect, driven by the conduction electrons, accounts for the above-described observations. They calculated the Hamiltonian for the system, assuming the intra-atomic Hund interaction (J_H^0) of the oxygen to have a significant value, while the energy Δ for excitation of the O(2p) electrons to the empty e_g levels of the localized Mn ions is small. Therefore, when an external pressure is applied, Δ increases, while the intra-atomic parameter J_H^0 remains unchanged, inducing the observed decrease of T_C.

In order to shed some light on the transport and magnetic mechanisms of this interesting material, several families of substituted compounds have been prepared, by chemical substitution in either Tl or Mn sublattices. The Tl has been partially replaced by In [2], Bi [6], Cd [7], and Pb [8]; the Mn sublattice has been doped with Ru [9], Sb [10], and Te [11]. In some cases, spectacular variations of the magnetotransport properties have been described. Perhaps the most dramatic change is produced in the $Tl_{2-x}Cd_xMn_2O_7$ series, where a magnetoresistance of 10^6 has been found for the $x = 0.2$ compound.

It is interesting to note the observation of an enhancement in the number of carriers and the ferromagnetic interactions in the Sb- and Te-substituted families, in direct relation to the mechanism of the magnetic interactions. In both series, the host cations are introduced into the manganese (Mn^{4+}) sublattice, and both cations have a higher nominal valence (Sb^{5+}, Te^{6+}) than Mn^{4+}. Therefore, the presence of a simultaneous electron-doping effect, leading to a partial reduction of manganese to Mn^{3+}, is very likely. Therefore, the enhancement of the FM interactions could be due to an additional mechanism of double exchange between neighbouring Mn^{3+} and Mn^{4+} cations. To deconvolute the effects of (i) introduction of a non-magnetic cation in the Mn sublattice and (ii) electron-doping effects due to change of valence, we have designed a new substitution with a non-magnetic tetravalent cation, commonly found in the B sublattice of pyrochlore-like structures: Ti^{4+}.

In this paper we report on the preparation and characterization of the Ti-substituted family $Tl_2Mn_{2-x}Ti_xO_7$ ($x = 0$, 0.2, and 0.4). We describe the results of a neutron diffraction study, and measurements of transport and magnetotransport properties and the Hall effect. We show that the replacement of manganese by titanium produces an enhancement in the number of carriers, but slightly reduces the strength of the magnetic interactions; the electrical resistance and magnetoresistance are also reduced with respect to the undoped compound.

2. Experimental procedure

$Tl_2Mn_{2-x}Ti_xO_7$ ($x = 0$, 0.2, and 0.4) pyrochlores were prepared under moderate pressure conditions. Stoichiometric amounts of the corresponding oxides (Tl_2O_3, MnO_2, and TiO_2)

were mixed and sealed into a gold capsule, which was placed inside a graphite heater. The reactions were carried out at 1000 °C and 2 GPa for 2 h, in a piston–cylinder hydrostatic press.

The products of the reactions were dense black homogeneous pellets. A fraction of the raw products were partially ground for use in the structural and magnetic characterization. Some as-grown pellets were kept for the magnetotransport measurements. The reaction products were characterized by means of x-ray diffraction (XRD) with Cu Kα radiation. A room temperature high-resolution neutron powder diffraction (NPD) pattern for the $x = 0.2$ sample was collected at the D2B diffractometer of the Institut Laue–Langevin, Grenoble, with a wavelength $\lambda = 1.594$ Å. The counting time for about 0.8 g of sample was four hours in the high-flux mode. NPD data were refined by the Rietveld method, using the FULLPROF refinement program [12]. A pseudo-Voigt function was chosen to generate the line shape of the diffraction peaks. In the final run the following parameters were refined: scale factor, background coefficients, zero-point error, unit-cell parameter, pseudo-Voigt function corrected for asymmetry parameters, positional coordinates (u for oxygen), isotropic thermal factors, and occupancy factors, for Tl and O′ oxygen.

The dc magnetic susceptibility was measured with a commercial SQUID magnetometer using powdered samples. The transport and magnetotransport measurements were performed under magnetic fields up to 9 T in a Physical Properties Measurement System (PPMS) from Quantum Design. The resistance and magnetoresistance (MR) were measured by the conventional four-probe technique, and the Hall effect was measured in the Hall-bar configuration, with five points, to compensate for the longitudinal component of the resistance. After that, a half of the difference between the positive and the negative branches of the transverse resistance was taken as the Hall resistance.

3. Results and discussion

The reaction products were characterized by means of XRD, and the reflections indexed in a cubic unit cell. The inset of figure 1 displays the variation in the unit-cell parameter a through

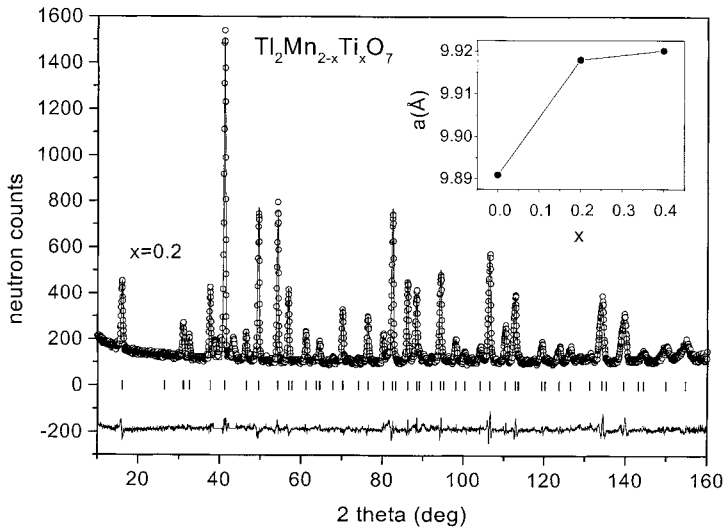

Figure 1. Observed (circles), calculated (full line), and difference (bottom) NPD Rietveld profiles for $Tl_2Mn_{1.8}Ti_{0.2}O_7$ at 295 K. Inset: variation of the lattice parameter with the Ti substitution (x).

the series; it increases with x, from $a = 9.9004(1)$ Å for $Tl_2Mn_2O_7$ to $a = 9.9201(1)$ Å for $Tl_2Mn_{1.6}Ti_{0.4}O_7$. This variation is consistent with the larger ionic radius for Ti^{4+} (0.605 Å) compared to that for Mn^{4+} (0.53 Å). The relatively small increment of the unit-cell parameter from $x = 0.2$ to $x = 0.4$ oxides suggests that the maximum Ti substitution admitted by the pyrochlore is lower than 0.4; assuming a linear variation of a with the actual Ti content, it can be estimated as 0.28 for the nominal $x = 0.4$ compound. In fact, a substantial variation of the macroscopic properties has also been observed for this member, and, hence, it has been included in this report.

Table 1 lists the structural parameters after the Rietveld refinement of the NPD pattern for $x = 0$ and 0.2 compounds. Figure 1 shows the quality of the fit of the $x = 0.2$ material. The pyrochlore structure, of crystallographic formula $A_2B_2O_6O'$, can be described as two interpenetrating networks [14], B_2O_6 and A_2O'; the latter is not essential for the stability of the structure: both A and O′ atoms may be partially or totally absent, as happens in certain families of defect pyrochlores AB_2O_6 [14]. The refinement of the occupancy factors for Tl and O′ led to stoichiometries significantly deficient in both atomic positions for the pure compound, but fully stoichiometric in O′ and Tl for the Ti-substituted material: the respective crystallographic formulae can be written as $Tl_{1.94(1)}Mn_2O_6O'_{0.96(1)}$ for $x = 0$ and $Tl_{1.98(1)}Mn_{1.8}Ti_{0.2}O_6O'_{1.01(1)}$ for $x = 0.2$. The presence of vacancies of both kinds in the pure compound is probably associated with the moderate pressure conditions employed for the synthesis. However, it is important to underline that the Ti-doped oxide is not defective in the Tl and O′ sublattice, which is certainly associated with the much higher stability of Ti^{4+} versus Mn^{4+} cations: while

Table 1. Structural parameters for $Tl_2Mn_{2-x}Ti_xO_7$ obtained after the Rietveld refinement of NPD data at RT. Space group $Fd3m$; $Z = 8$.

	Nominal x	
Parameter	0	0.2
a (Å)	9.89090(6)	9.9179(1)
V (Å^3)	967.63(1)	975.57(1)
Tl 16c (0 0 0)		
B (Å^2)	0.62(2)	0.74(4)
f_{occ}	0.972(3)	0.972(4)
Mn, Ti 16d (1/2 1/2 1/2)		
B (Å^2)	0.45(3)	0.38(8)
O 48f (u 1/8 1/8)		
u	0.42484(7)	0.4248(1)
B (Å^2)	0.66(2)	0.84(3)
O′ 8a (1/8 1/8 1/8)		
B (Å^2)	0.35(4)	0.67(9)
f_{occ}	0.960(6)	1.00(1)
Crystallographic formula	$Tl_{1.944(6)}Mn_2O_{6.96(1)}$	$Tl_{1.98(1)}Mn_{1.8}Ti_{0.2}O_{7.00(1)}$
Reliability factors		
χ^2	1.81	2.28
R_p	4.06	5.40
R_{wp}	5.25	6.87
R_{exp}	3.90	4.55
R_I	2.15	4.74

Mn^{4+} requires high oxygen pressure to be stabilized in many oxides, Ti^{4+} is perfectly stable in air under ambient conditions.

This structural feature has important electronic consequences: the deficiency of Tl atoms is related to a certain degree of hole doping (or removal of electrons) in the 'undoped' compound, which is, indeed, thallium deficient. The Ti-substituted compounds are not Tl deficient (as shown from NPD data); thus the above-mentioned hole-doping effect is no longer present; this fact leads to a net increase of the number of carriers (electrons) in the Ti-doped phases. The refinement of the corresponding Mn/Ti ratio in the pyrochlore structure was not possible from NPD data, given the similarity of their scattering lengths. The Mn–O distance observed for $Tl_2Mn_2O_7$, of 1.9016(1) Å, slightly increases for $Tl_2Mn_{1.8}Ti_{0.2}O_7$, with $d_{Mn-O} = 1.9052(7)$ Å; this is consistent with the larger ionic radius of Ti^{4+} versus Mn^{4+}. The Mn–O–Mn angles (133.9(1)°) are almost unchanged upon doping.

The dc susceptibility curves, measured under 0.1 T and after a field-cooling process, are shown in figure 2. The curves correspond to FM compounds, with a transition to the

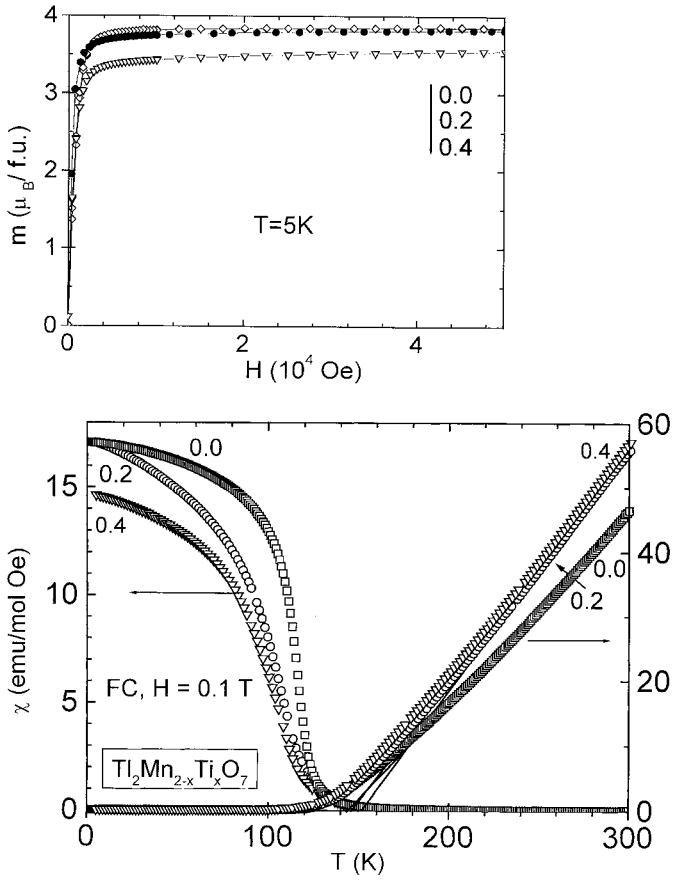

Figure 2. Main (bottom) panel: susceptibility (left-hand axis) versus temperature curves for $Tl_2Mn_{2-x}Ti_xO_7$, measured after a zero-field-cooling process, under a magnetic field of 0.1 T. The right-hand axis gives the inverse susceptibility. Note that, when lowering the temperature from high values, there is a deviation from the Curie–Weiss linear behaviour for all the samples, explained by the formation of spin polarons. Top panel: magnetization per formula unit versus applied magnetic field, measured at 5 K, for the samples.

paramagnetic state near 120 K. T_C is slightly lowered upon doping, as can be seen in table 2. The right-hand axis of figure 2 shows the inverse of the susceptibility. In the paramagnetic region above T_C, a Curie–Weiss fit leads to the Weiss temperatures θ_W given in table 2. In the top panel the 5 K magnetization versus field curves are shown. Again these data correspond to FM materials, the value of the saturation magnetization being lowered upon doping (see also table 2). This decrease in the saturation magnetization upon doping, also observed in the paramagnetic moment (μ_{eff}), is consistent with the fact that the magnetic Mn^{4+} cations are partially removed, and replaced by non-magnetic Ti^{4+} cations.

Table 2. Main magnetic and transport parameters of the Ti-doped $Tl_2Mn_2O_7$ compounds.

x	T_C (K)	M_s (μ_B)	μ_{eff} (μ_B)	Θ_W (K)	ρ_{RT} (Ω cm)	E_σ (meV)	C
0.0	118	3.83	5.37	154	25.7	55.4(6)	48.4
0.2	110	3.77	4.64	155	0.15	26.1(1)	6.9
0.4	110	3.45	4.43	165	0.03	26.1(1)	5.3

As in other $Tl_2Mn_2O_7$-related compounds, the linear paramagnetic behaviour of the inverse of the susceptibility is exhibited only for relatively high temperatures, while for temperatures immediately above and around T_C the curve deviates from the expected paramagnetic behaviour. This has been attributed to the existence of magnetic polarons, up to temperatures as high as about $2T_C$.

In figure 3, we show the thermal variation of the resistivity, without applied magnetic field (solid symbols) and with an external magnetic field of 9 T (open symbols). In the absence of a magnetic field, a metal-to-insulator transition is observed for all the samples around T_C. On heating, this transition displays an enhancement of the resistivity, of about one to two orders of magnitude. The increment in the resistance is due to the disordering in the magnetic moments that takes place above T_C. This provokes an increment of the magnetic scattering, due to the strong polarization of the charge carriers.

On applying a magnetic field, the resistivity significantly drops and the metal–insulator transition is moved to higher temperatures. This is reflected in the value of the magnetoresistance, defined as $\mathrm{MR}(H) = [\rho(0\ \mathrm{T}) - \rho(H)]/\rho(0\ \mathrm{T})$ (see the top panel). Upon doping with Ti, there is a clear reduction of the resistivity, by about three orders of magnitude at room temperature, and about one order at low temperatures. This reduction upon doping is probably related to the increase in the number of carriers, as will be commented on below. It is striking that for the doped compound the difference between the high-temperature and low-temperature values of the resistivity is lower than in the pure undoped compound. This is attributable to the lower degree of ordering of the magnetic lattice in the case of the doped compounds, since we are replacing magnetic Mn^{4+} cations with non-magnetic Ti^{4+} ones. Therefore, the difference in magnetic scattering between the low-temperature, ferromagnetically ordered state and the high-temperature, disordered state will be lower. The same feature lies at the origin of the smaller difference in resistivity when a magnetic field is applied in the Ti-doped compounds. This is reflected in a lower value for the MR, as can be seen in the top panel.

The conductivity in the region above T_C follows a thermally activated behaviour, suggesting the existence of magnetic polarons in this temperature regime. As proposed by Chun *et al* [15], when the transport is driven by polaron hopping the conductance takes the form

$$\sigma_{xx} = \frac{1}{\rho_{xx}} = \sigma_0 \exp\left(-\frac{E_\sigma}{k_B T}\right)$$

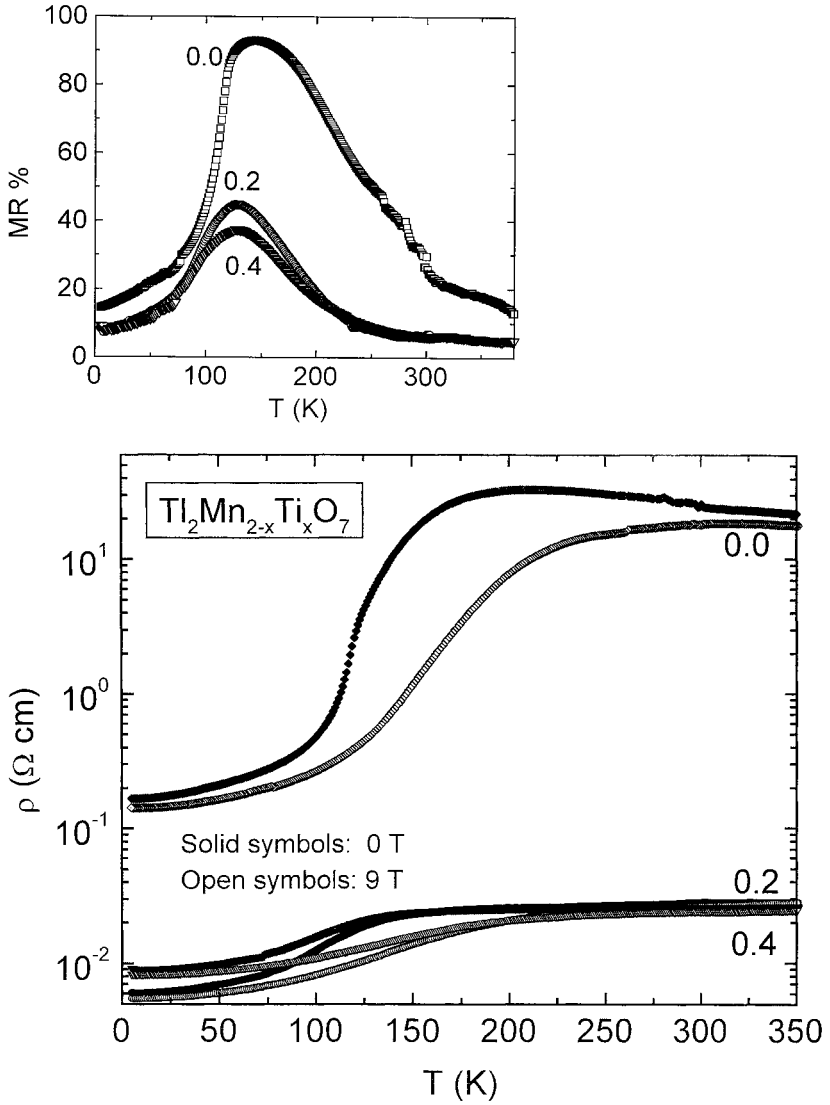

Figure 3. Main (bottom) panel: variation of the resistance with temperature for $Tl_2Mn_{2-x}Ti_xO_7$, with (open symbols) and without (solid symbols) a 9 T magnetic field applied. There is a metal–insulator transition for all the samples, together with a reduction in the resistance upon the application of the magnetic field. Top panel: the magnetoresistance versus temperature. One can see that the peak in the MR appears around T_C.

where $\sigma_0 = g_d e^2 \nu_0 \delta / a k_B T$. The factor g_d is determined by the hopping geometry; ν_0 and a are the attempt frequency and hopping distance, respectively, and δ is the carrier concentration per Mn site. The values obtained for the activation energy E_σ are given in table 2. The observed decrease of the activation energy for the Ti-doped compounds is in agreement with a lower saturation magnetization value. If we consider a magnetic polaron as a cluster of neighbouring magnetic cations with ferromagnetic alignment of spins, the energy necessary to align the moments of the Mn cations magnetically will be lower in the case of the Ti-doped compounds, as Ti^{4+} cations are distributed at random in the Mn sublattice.

Majumdar and Littlewood proposed a model for the high-temperature resistance of a FM material with a low density of carriers [16]. According to their model, transport above about $1.2\,T_C$ is governed by polaron hopping, showing a scaling between the MR and the square of the magnetization, independently of the temperature:

$$\frac{\rho(H) - \rho(H=0)}{\rho(H=0)} = C(M/M_s)^2.$$

Figure 4 shows the MR values versus the square of the magnetization, for three different temperatures: 200, 250, and 300 K. There is a good agreement between the experimental data and the above-mentioned model, suggesting, once again, that the electronic transport in this temperature range is governed by magnetic polaron hopping. Moreover, Majumdar and Littlewood gave a relation between the scaling factor C and the number of carriers: $|C| \approx n^{-2/3}$. C-values are given in table 2. $|C|$-values diminish as the Ti substitution increases, as expected for a higher density of carriers. This is in complete agreement with the lower values found for the resistivity in the Ti-doped compounds.

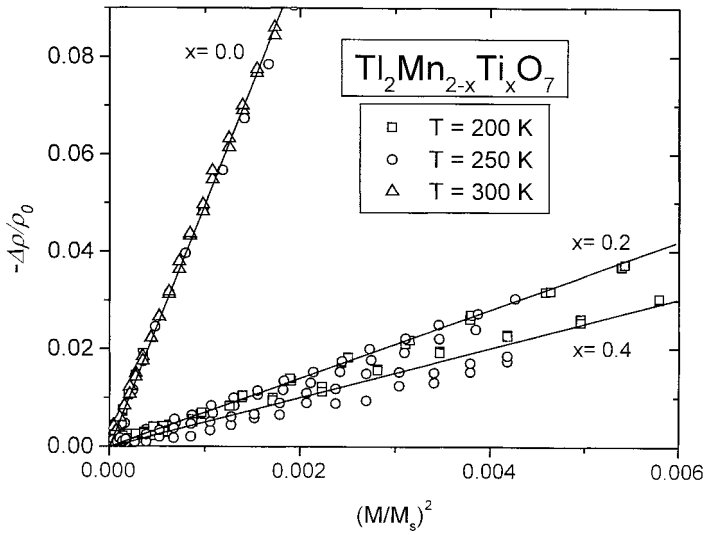

Figure 4. Magnetoresistance versus the square of the magnetization normalized to the saturation value, at 200 K (squares), 250 K (circles), and 300 K (triangles). The good agreement with the Majumdar–Littlewood model is clear [16]. A lower slope corresponds to an increase in the number of carriers.

Hall-effect measurements were performed under applied fields up to 9 T. The slopes of the Hall resistivity show that the carriers are electrons, as is also the case for other $Tl_2Mn_2O_7$ derivatives. There is an enhancement in the density of electrons, from 7.7×10^{-4} for the pure compound to approximately 2×10^{-2} for the $x = 0.4$ substituted compound. This result is in good agreement with the behaviour expected from the Majumdar–Littlewood model, predicting a reduction of C and, thus, an increase in the number of carriers for the Ti-doped samples.

As deduced from the NPD data, the increase of the number of carriers (electrons) in the Ti-substituted materials is related to the absence non-stoichiometry of the pyrochlore, with respect to the undoped compound. In fact, the so-called 'undoped' $Tl_2Mn_2O_7$ pyrochlore has been demonstrated to show a measurable Tl deficiency [17] and, therefore, a hole-doping effect, implying a reduction in the number of electrons. This deficiency is related to the

moderate pressures used for the synthesis of this compound, requiring extreme conditions for the stabilization of the fully stoichiometric material. The introduction of Ti leads to a net stabilization of the pyrochlore phase, in such a way that the non-stoichiometry is significantly reduced. For the 'undoped' compound, the introduction of Ti plays the role of electronic injection, in spite of the homovalent character of Mn^{4+} and Ti^{4+}.

Finally, it is worth making a comparison between the present results obtained for the Ti-substituted series and those previously reported for the Sb^{5+}- and Te^{6+}-doped compounds. For all three chemical derivatives, an increase in the number of carriers upon doping (as reinforced by Hall-effect and Majumdar–Littlewood model measurements) has been reported. The main difference lies in the enhancement of the ferromagnetic interactions observed in the Sb and Te pyrochlores (as shown by susceptibility measurements), while for the Ti samples the ferromagnetism is slightly reduced. According to Núñez-Regueiro and Lacroix's model, the driving mechanism for the FM interaction in $Tl_2Mn_2O_7$ is a superexchange between neighbouring Mn ions, while the O′ states do not participate in the superexchange FM coupling. Therefore, an increase in the number of carriers in the Mn bands (strongly hybridized with Tl 6s and O 2p orbitals) would enhance the FM interactions, as happens in the Sb^{5+}- and Te^{6+}-doped compounds, in which an electronic injection is achieved in bands of Mn parentage. In the case of the Ti^{4+} pyrochlores, the extra carriers are injected at the O′ positions, which overlap poorly with the 3d Mn bands, as shown from electronic band calculations, in such a way that the injected electrons are able to participate in the electronic conduction (decrease of resistivity and MR) but have little influence on the magnetic interactions, which are mediated by electrons residing in bands of Tl–Mn–O character. In contrast, the presence of non-magnetic Ti^{4+} cations in the magnetic Mn^{4+} sublattice spoils the ferromagnetic interactions, leading to a decrease of the Curie temperatures and the saturation magnetic moments.

4. Conclusions

In this work we have prepared, measured, and explained the magnetotransport properties of a new manganese pyrochlore family: $Tl_2Mn_{2-x}Ti_xO_7$. With respect to the undoped compound, there is an enhancement in the number of carriers (as demonstrated by Hall-effect measurements and agreement with the Majumdar–Littlewood model [16]), in bands of Tl parentage, which are responsible for a decrease in the resistivity, while the magnetism is almost unchanged. This is consistent with the scenario given by Núñez-Regueiro and Lacroix [5], in which an extra FM indirect exchange term, explaining the abnormally high Curie temperatures observed in $Tl_2Mn_2O_7$ pyrochlore, depends upon conduction electrons localized in bands resulting from the strong hybridization of Mn 3d, Tl 6s, and O 2p orbitals.

Acknowledgments

We are grateful for the financial support from MCyT given to the projects MAT2001-0539 and MAT99-1045, and we are grateful to the ILL for making facilities available.

References

[1] Shimakawa Y, Kubo Y and Manako T 1996 *Nature* **379** 53
[2] Cheong S-W, Hwang H Y, Batlogg B and Rupp L W 1996 *Solid State Commun.* **98** 163
[3] Subramanian M A, Toby B H, Ramirez A P, Marshall W J, Sleight A W and Kwei G H 1996 *Science* **273** 81
[4] Sushko Yu V, Kubo Y, Shimakawa Y and Manako T 1999 *Physica* B **259–261** 831
[5] Núñez-Regueiro M D and Lacroix C 2001 *Phys. Rev.* B **63** 14 417

[6] Alonso J A, Martínez J L, Martínez-Lope M J, Casais M T and Fernández-Díaz M T 1999 *Phys. Rev. Lett.* **82** 189
[7] Alonso J A, Velasco P, Martínez-Lope M J, Casais M T, Martínez J L, Fernández-Díaz M T and de Paoli J M 2000 *Appl. Phys. Lett.* **76** 3274
[8] Velasco P, Alonso J A, Martínez-Lope M J, Casais M T and Martínez J L 2001 *J. Magn. Magn. Mater.* at press
[9] Senis R *et al* 2000 *Phys. Rev.* B **61** 11 637
and see also
Martínez B *et al* 1999 *Phys. Rev. Lett.* **83** 2022
[10] Alonso J A, Martínez-Lope M J, Casais M T, Velasco P, Martínez J L, Fernández-Díaz M T and de Paoli J M 1999 *Phys. Rev.* B **60** R15 024
[11] Velasco P, Alonso J A, Martínez-Lope M J, Casais M T, Martínez J L, Fernández-Díaz M T and de Paoli J M 2001 *Phys. Rev.* B **64** 184436
[12] Rodríguez-Carvajal J 1993 *Physica* B **192** 55
[13] Shannon R D 1976 *Acta Crystallogr.* A **32** 751
[14] Subramanian M A, Aravamudan G and Subba Rao G V 1983 *Prog. Solid State Chem.* **15** 55
[15] Chun S H, Salamon M B, Tomioka Y and Tokura Y 2000 *Phys. Rev.* B **61** R9225
[16] Majumdar P and Littlewood P B 1998 *Nature* **395** 479
[17] Alonso J A, Martínez-Lope M J, Casais M T, Martínez J L and Fernández-Díaz M T 2000 *Chem. Mater.* **12** 1127